Cell, Vol. 111, 29–40, October 4, 2002, Copyright ©2002 by Cell Press

The Role of Apoptosis in Creating and Maintaining Luminal Space within Normal and Oncogene-Expressing Mammary Acini

Jayanta Debnath,[1,2] Kenna R. Mills,[1] Nicole L. Collins,[1] Mauricio J. Reginato,[1] Senthil K. Muthuswamy,[1,4] and Joan S. Brugge[1,3]
[1]Department of Cell Biology
Harvard Medical School
Boston, Massachusetts 02115
[2]Department of Pathology
Brigham and Women's Hospital
Boston, Massachusetts 02115

Summary

We have utilized in vitro three-dimensional epithelial cell cultures to analyze the role of apoptosis in the formation and maintenance of a hollow glandular architecture. Lumen formation is associated with the selective apoptosis of centrally located cells; this apoptosis follows apicobasal polarization and precedes proliferative suppression during acinar development. Notably, either inhibiting apoptosis (by exogenously expressing antiapoptotic Bcl family proteins) or enhancing proliferation (via Cyclin D1 or HPV E7 overexpression) does not result in luminal filling, suggesting glandular architecture is resistant to such isolated oncogenic insults. However, the lumen is filled when oncogenes that enhance proliferation are coexpressed with those that inhibit apoptosis, or when ErbB2, which induces both activities, is activated by homodimerization. Hence, apoptosis can counteract increased proliferation to maintain luminal space, suggesting that tumor cells must restrain apoptosis to populate the lumen.

Introduction

Glandular epithelium, such as in the mammary gland, is comprised of individual acinar units, which are notable for a hollow lumen, surrounded by polarized epithelial cells. The development and maintenance of this polarized structure is critical for the form and function of epithelial cells, both in maintaining a differentiated state and in the control of cell proliferation and cell survival (Bissell and Radisky, 2001). Furthermore, the pathogenesis of carcinoma requires the disruption of this intact, well-ordered architecture. Notably, filling of the luminal space is a hallmark of early epithelial tumors, such as atypical hyperplasias and ductal carcinoma in situ (DCIS) in the breast (Harris et al., 1999). However, very little is known about how the lumen in a glandular epithelial structure is normally formed and maintained as well as what processes lead to the population of the lumen during tumor development. This information should provide biological insight into carcinoma progression and help create a mechanistic framework in the search for new diagnostic markers and therapeutic targets in epithelial cancers.

Three-dimensional (3D) basement membrane cultures provide a unique opportunity to model the architecture of epithelium in vitro (O'Brien et al., 2002). Unlike monolayer cultures, mammary epithelial cells grown in 3D recapitulate numerous features of breast epithelium in vivo, including the formation of growth-arrested polarized acini with a hollow lumen and basal deposition of basement membrane components, such as collagen IV and laminin V (Gudjonsson et al., 2002; Petersen et al., 1992; Streuli and Bissell, 1990; Weaver et al., 2002). Thus, 3D epithelial cultures provide the appropriate structural and functional context fundamental for studying the events involved in morphogenesis of glandular epithelium as well as for modeling the biological activities of cancer genes. Furthermore, because mammary epithelial acini grown in 3D matrices are amenable to biochemical and cell biological analysis, they also provide the opportunity to study the molecular mechanisms necessary to form and maintain a normal glandular architecture and to determine how cancer genes disrupt this hollow, polarized architecture. For example, our laboratory has recently shown that activating ErbB2/Her2, an oncoprotein of the epidermal growth factor receptor (EGFR) family involved in mammary cancer, reinitiates proliferation in preformed MCF-10A mammary epithelial acini and generates complex multiacinar structures; these altered structures exhibit many of the properties of early-stage epithelial tumors, including a high level of proliferation, filling of the lumen, deposition of a basement membrane, and the lack of invasive properties (Muthuswamy et al., 2001).

The striking degree of luminal filling in these structures prompted us to further investigate the creation and maintenance of luminal space in mammary acini, both normally and in the context of a proliferative stress imposed by an oncogene. Apoptosis has previously been implicated in lumen formation. The importance of programmed cell death in cavitation was first recognized during the formation of the proamniotic cavity in the vertebrate embryo (Coucouvanis and Martin, 1995, 1999). Subsequently, the presence of apoptotic cells in the lumen has been noted in several other in vitro spheroid systems, including salivary gland cysts and endothelial and mammary spheroids (Blatchford et al., 1999; Hoffman et al., 1996; Korff and Augustin, 1998). However, a lumen can also be created independently of apoptosis (O'Brien et al., 2002). For example, when small clusters of Madin-Darby Canine Kidney (MDCK) epithelial cells become polarized, the separation of opposing apical membranes results in the generation of a small lumen (Ojakian et al., 1997). Although polarization and apoptosis both appear to play important roles in creating a lumen, the temporal coordination and relative importance of these processes remains uncertain in mammary acinar morphogenesis. Furthermore, how cancer genes modulate these processes within three-dimensional structures has not been extensively investigated.

In this study, we have focused on the role and require-

[3]Correspondence: joan_brugge@hms.harvard.edu
[4]Present address: Cold Spring Harbor Laboratory, 1 Bungtown Road, Cold Spring Harbor, New York 11274.

ment of apoptosis in the formation and maintenance of luminal space during the in vitro morphogenesis of both normal and oncogene-expressing mammary epithelial acini. We have found that cells in direct contact with basement membrane become polarized prior to bona fide lumen formation. After this apicobasal polarity is established and prior to growth arrest, the centrally located nonpolarized cells are cleared by apoptosis to form a hollow lumen. Overexpressing Bcl-2 or Bcl-X_L in acini inhibits luminal apoptosis and delays clearance of cells from the developing luminal space. However, these structures eventually do form a hollow lumen, indicating that other processes contribute to lumen formation.

Although apoptosis is not a requisite in creating luminal space, it is necessary to maintain a hollow lumen when enhanced oncogenic proliferation occurs within an acinus. Acini expressing proliferative oncoproteins such as cyclin D1 and human papilloma virus (HPV) 16 E7 escape proliferative suppression but have hollow lumen because excess cells die in the luminal space. In contrast, mammary structures with activated ErbB2 are filled and display reduced levels of luminal apoptosis. Overall, these results illustrate that tumor cells must overcome apoptosis in order to populate the lumen of in vitro mammary epithelial structures and point to the utility of this three-dimensional culture system in elucidating the requirements for architectural disruption during early carcinoma formation.

Results

Lumen Formation during Mammary Epithelial Acini Morphogenesis

The three-dimensional culture of MCF-10A cells, a nontransformed mammary epithelial cell line, can be used to model the biological properties of oncogenes (Muthuswamy et al., 2001). When cultured on a reconstituted basement membrane derived from Engelbreth-Holm-Swarm tumor (Matrigel™), MCF-10A cells undergo a series of proliferative and morphogenetic events resulting in the formation of growth-arrested acini-like spheroids, composed of a single layer of polarized epithelial cells surrounding a hollow lumen; this lumen becomes evident after 10 to 12 days in three-dimensional (3D) culture and remains hollow thereafter (Muthuswamy et al., 2001). As discussed above, both apoptosis and apicobasal polarization have been implicated in the formation of a hollow lumen in epithelial structures. In order to better understand how normal MCF-10A acinar structures are formed and establish a time course of key morphogenetic events that could be subject to dysregulation by cancer genes, we examined the contributions of polarization and apoptosis to acinar morphogenesis.

Apicobasal polarization was monitored during morphogenesis by immunostaining for the α6 integrin subunit and the *cis*-Golgi protein GM130. In polarized epithelia, α6 integrin is located on the basal surface, whereas GM130 assumes an apical location. By days 3 and 4 in 3D culture, we observed the polarized location of both α6 integrin and GM130 (Figure 1, right and center columns). These cell clusters also basally secreted a basement membrane during early time points, which we were able to detect by immunostaining with antibodies that specifically recognized the human isoforms of laminin V (left column) and collagen IV (data not shown). In addition, these cell clusters displayed the cell-cell junction localization of E-cadherin and β-catenin (data not shown). Thus, apicobasal polarity is established very early in the morphogenetic process, prior to the formation of a bona fide lumen. Notably, at days 5 through 8 in culture, we were able to discern two populations of cells within each acinus, a well-polarized outer layer of cells that was in direct contact with matrix and an inner subset of cells that was poorly polarized and lacking contact with the matrix. At later time points, this inner population of cells was absent, and each acinar structure exhibited a hollow lumen surrounded by a well-polarized layer of cells.

Two lines of evidence corroborated the presence of cell death in mammary epithelial acini (Figure 2). First, acini were treated in situ with ethidium bromide (a DNA intercalating dye that cannot enter living cells with intact plasma membranes but can readily label dying cells whose membrane integrity has been compromised) and calcein AM (a fluorescent compound that is only metabolized by live cells). In mammary acini, dying ethidium bromide-positive cells were found only in the interior of the developing structures, whereas cells in direct contact with matrix were alive and stained positively for calcein AM (Figure 2A). Second, we established that the death occurring within an acinus involved type I apoptotic processes by immunostaining for an antibody directed against the cleaved, activated form of caspase-3. Once again, only cells in the presumptive luminal space stained positively for activated caspase-3; notably, many of these cells exhibited fragmented nuclei upon staining with the nuclear dye 4′,6-diamidino-2-phenylindole (DAPI) (Figures 2B and 2C). Similar results were obtained upon immunostaining with an antibody directed against activated caspase-9 (data not shown).

Cell death was first detected between days 6 and 8 of morphogenesis, continuing on thereafter (Figures 2D). Importantly, the onset of luminal apoptosis immediately preceded the appearance of hollow lumen in MCF-10A acini, which became evident by day 10 in 3D culture (Figure 2D). MCF-10A cells require several media components for proliferation and survival in both monolayer and three-dimensional culture, including epidermal growth factor (EGF), insulin, and hydrocortisone (Soule et al., 1990). In our standard assays, cultures were refed at 4 day intervals. In order to determine whether nutrient or growth factor deprivation secondary to our regular cell culture conditions contributed to apoptosis, we refed the cultures with fresh complete media on a daily basis. This increased frequency of feeding did not alter the temporal pattern of cell death (data not shown). Furthermore, upon treating acini with flourescein-labeled dextrans of various sizes, we observed that cells in the luminal space had access to molecules as large as 40 kDa (data not shown). Altogether, these results suggest that luminal apoptosis is not secondary to cell culture conditions or deficient access to growth and survival factors; rather, it is part of an established morphogenetic program during acinar development.

The selective apoptosis of centrally located cells prompted us to explore the signals that might contribute to the survival of cells occupying the periphery of these

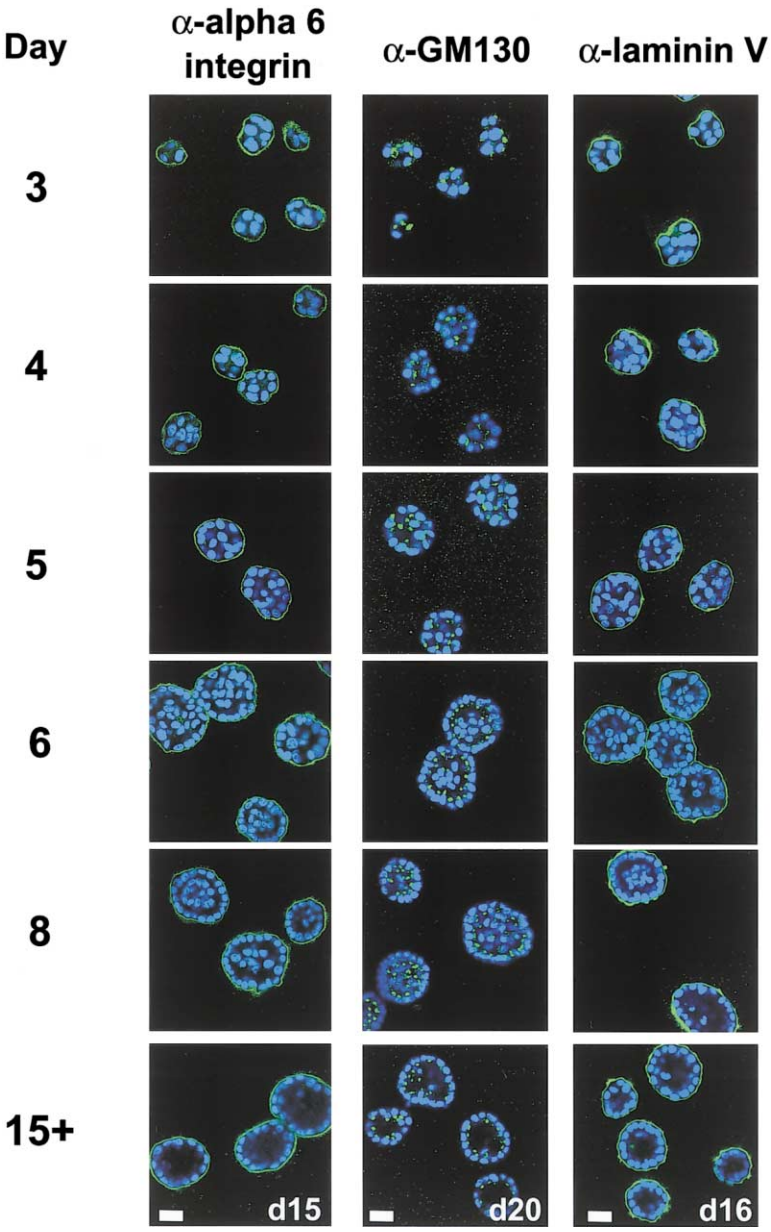

Figure 1. Apicobasal Polarity Is Established Prior to Lumen Formation in MCF-10A Mammary Epithelial Acini

MCF-10A cells were cultured on Matrigel for the indicated number of days (d). Representative confocal images of crosssections through the middle of acini are shown with the nuclei counterstained with DAPI (blue). Developing acini were immunostained with antibodies to the α_6 integrin subunit (green, right), the *cis*-Golgi protein GM130 (green, center), and laminin V (green, left). Bars equal 25 μm.

structures. Akt is a serine-threonine kinase whose activation by growth factors and extracellular matrix receptors provides survival signals by phosphorylating several proteins, including the proapoptotic BH3 protein, BAD, and the Forkhead family of transcription factors (Brunet et al., 1999; Datta et al., 1997, 1999). We examined the spatial pattern of Akt kinase activation within developing mammary acini by immunostaining with two different phospho-specific antibodies—one that recognizes an activation-specific phosphorylation site in Akt (α-P-Akt Ser^{473}; Figure 3, top) and a second that recognizes the phosphorylated consensus motif (RxRxxpS/T) of Akt substrates (α-P-Akt substrate; Figure 3, bottom; Manning et al., 2002; Watton and Downward, 1999). These studies indicated that both phospho-Akt and its phosphorylated substrates were present in a stochastic pattern confined to the peripheral matrix-attached cells of acini. In contrast, Akt pathway activation was not detected in the centrally located, nonpolarized cells located in the developing luminal space of early structures (Figure 3, center). Overall, these data suggest that the centrally located cells in the developing lumen of early structures lack important survival signals provided by the Akt pathway, which may contribute to their selective cell death during lumen formation.

Proliferative Suppression Follows Lumen Formation during Acinar Morphogenesis

Previously, we had determined that the total cell numbers in three-dimensional cultures do not increase after day 6, suggesting that the acini had reached a "growth-arrested" state (Muthuswamy et al., 2001). We also found that acinar size reached a plateau; the mean diameter $\pm$ standard deviation of a structure after day 8

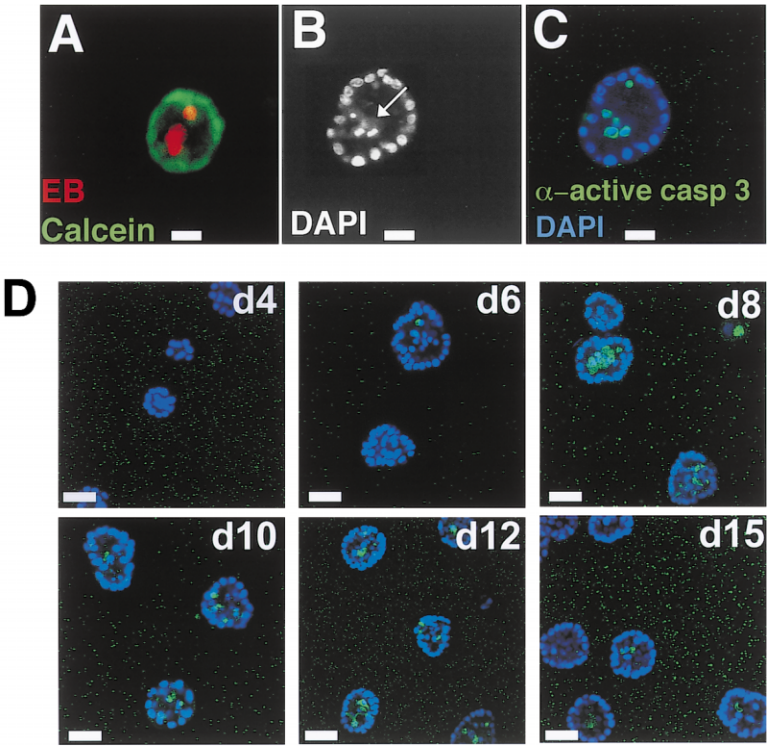

Figure 2. Luminal Apoptosis during Mammary Acinar Morphogenesis

(A) Acini grown in three-dimensional culture were stained with ethidium bromide (EB, orange) to mark dying cells and calcein AM (green) to label viable cells. A crosssection through the middle of a day 15 acinus shows cells dying in the luminal space, whereas cells lining the lumen remain viable. Bar equals 25 μm.

(B and C) DAPI-stained confocal crosssection through the middle of a day 12 structure shows cells in the luminal space with fragmented nuclei, characteristic of apoptosis (arrow, B). These cells also stain positively for the cleaved product of activated caspase-3 (green, C), indicating that these cells are undergoing apoptosis. Bars equal 25 μm.

(D) Developing acini were immunostained for activated caspase-3 (green) after culture for the indicated number of days (d). Increased caspase-3 activation is first detected in the luminal space at day 8 and continues thereafter. Bars equal 50 μm.

was 67.5 ± 13.4 μm (Figure 4A). Since luminal apoptosis continues after acinar size and cell numbers have stabilized, as well as after the formation of a hollow lumen (Figure 2D), we investigated if proliferation also continued within structures after size had stabilized by immunostaining with an antibody toward Ki-67, a nuclear protein that is only expressed during late G1 through M phase of the cell cycle (Scholzen and Gerdes, 2000). Using this commonly employed marker to detect proliferating cells (Figure 4B), we found that proliferation continued long after acinar size had reached a plateau. During the first 12 days, 90%–100% of acini in a 3D culture possessed two or more Ki-67-positive cells. In contrast, from day 15 onward, less than 20% of acini in a culture possessed Ki-67-positive cells; moreover, the individual acini in these late-stage cultures usually contained isolated Ki-67-positive cells in contrast to the structures from earlier time points (Figure 4B, compare days 15 and 20 to days 6 and 10). Thus, proliferative suppression in MCF-10A acini occurs several days after the onset of luminal apoptosis and the formation of a hollow lumen. Furthermore, proliferation, albeit at low levels, is always present within mammary acini; consequently, apoptosis may counterbalance sporadic proliferative events to maintain the size and hollow architecture of each acinus.

Based on these results, we speculated that apoptotic clearance contributes to two aspects of acinar morpho-

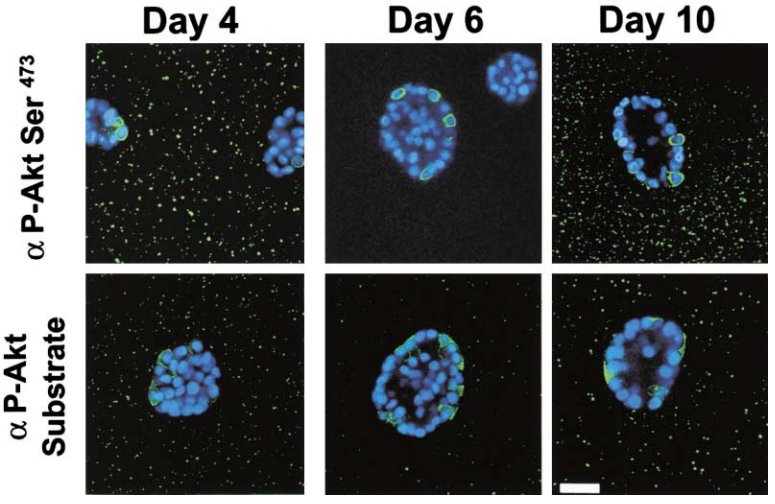

Figure 3. Akt Is Selectively Activated in the Polarized Outer Cells of Acini

Developing MCF-10A mammary acini, cultured in basement membrane for the indicated number of days, were fixed and immunostained with anti-phospho-Akt Ser^{473} (green, top) and anti-phospho-Akt substrate (green, bottom). Confocal DAPI-stained (blue) crosssections through the equators of acini are shown. Bars equal 25 μm.

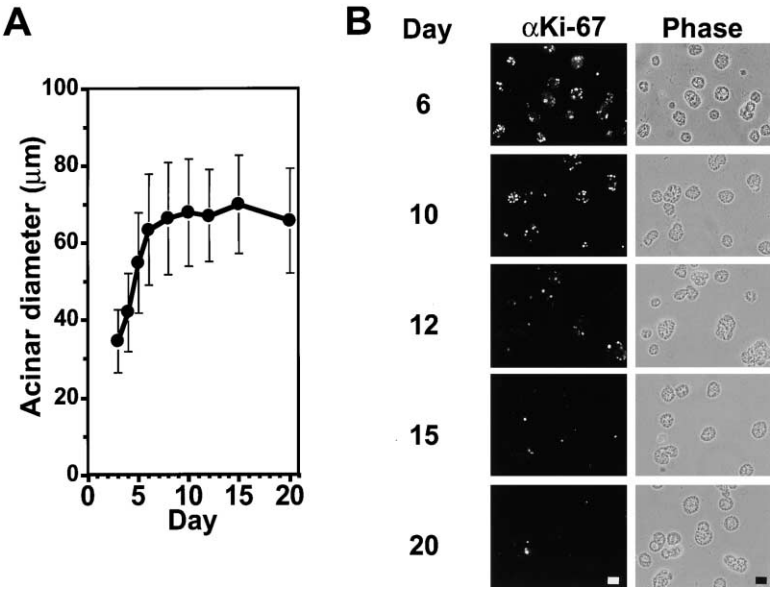

Figure 4. Proliferative Suppression in Mammary Acini

(A) The mean (± standard deviation) diameters of MCF-10A acini after the indicated days in basement membrane culture are shown. For each time point, the diameters through the largest confocal crosssection of 100–120 structures were measured using a micrometer.

(B) Acini were cultured in Matrigel for the indicated number of days, fixed, and immunostained with antibody against Ki-67. Representative fields show decreasing numbers of Ki-67-positive cells within acini starting at day 12 (row 3), with occasional Ki-67-positive cells detected in day 15 and 20 acini (rows 4 and 5). The corresponding phase contrast images are shown in right column. Bars equal 50 μm.

genesis. First, luminal apoptosis is involved in the clearance of cells during the generation of the hollow lumen in acini. Second, apoptosis can eliminate proliferating cells that are deposited into the luminal space during and after lumen formation. Thus, luminal apoptosis can potentially counteract an increase in proliferation, including that provided by a cancer gene, and maintain an intact, hollow glandular architecture.

Inhibiting Apoptosis Delays but Does Not Prevent the Formation of a Hollow Lumen in Normal MCF-10A Acini

In order to assess whether apoptosis was functionally required for lumen formation, stable pools of MCF-10A cells overexpressing the antiapoptotic proteins Bcl-2 and Bcl-X_L were established and these cells were cultured on basement membrane. To quantify the extent of luminal apoptosis occurring in a culture at various time points, we determined the percent of acini in the total culture that contained one or more ethidum bromide-positive cells in the lumen (Figures 5A and 5B). Luminal apoptosis was significantly reduced in cells overexpressing either Bcl-2 or Bcl-X_L: only 15% of these structures exhibited ethidium bromide-positive cells at day 8; in contrast, 65% of the acini in control cultures exhibited ethidium bromide-positive cells in the luminal space (Figure 5A). In addition, activated caspase-3 was not detected in the luminal space of Bcl-2- and Bcl-X_L-expressing structures (Figure 5C and data not shown).

Furthermore, we examined the effects of inhibiting luminal apoptosis on the formation of a hollow lumen in mammary acini. DAPI-stained crosssections through the middle of these acini showed that viable cells were present within the lumen of day 12 Bcl-2- and Bcl-X_L-expressing structures (Figure 5D and data not shown). In contrast, vector-infected (pBABE) controls at the same time points were hollow (Figure 5D). However, by day 16 in culture, the lumen of the Bcl-2 and Bcl-X_L acini were largely hollow, similar to that of controls (Figure 5D). This clearing occurred despite the fact that Bcl-2- or Bcl-X_L-expressing acini continued to display low levels of ethiduim bromide and caspase-3 staining throughout the culture process (Figures 5A and 5C and data not shown); moreover, expression of the Bcl proteins did not decrease over time (data not shown). Thus, although inhibiting apoptosis delays the clearance of cells from the luminal space during morphogenesis, it does not prevent lumen formation in MCF-10A acini. Previous studies in the mammary gland have suggested that Bcl-2 can have antiproliferative effects; accordingly, decreased proliferation during morphogenesis would result in fewer cells within a structure, which would obviate the need for apoptotic clearance of excess cells during lumen formation (Furth et al., 1999; Murphy et al., 1999). However, we did not observe decreased acinar size, cell number, or reduced rates of proliferation in Bcl-2- or Bcl-X_L-expressing structures during morphogenesis (data not shown).

To further understand the clearance process during lumen formation, we analyzed the ultrastructural morphology of both normal and Bcl-2-expressing structures by transmission electron microscopy. In day 8 MCF-10A acini, dying cells were present in the lumen (Figure 5E, image a, boxed area). The ultrastructure of these cells was notable for fragmented nuclei (white arrow) as well as an extensive network of cytoplasmic vacuoles (black arrows). Several of these vacuoles contained cytoplasmic matter and organelles within them, suggesting they are autophagic in nature (Figure 5E, image a′). Remarkably, these filled vacuoles were also present in the centrally located cells of Bcl-2-expressing acini (Figure 5E, images b and b′, black arrows), indicating that Bcl-2 does not inhibit this process. Notably, cytoplasmic vacuolation is a characteristic of alternative death processes, including autophagic death and paraapoptosis (Bursch et al., 2000; Leist and Jaattela, 2001; Sperandio et al., 2000). Overall, these ultrastructural studies indicate that lumen formation may involve alternative death processes, such as autophagy.

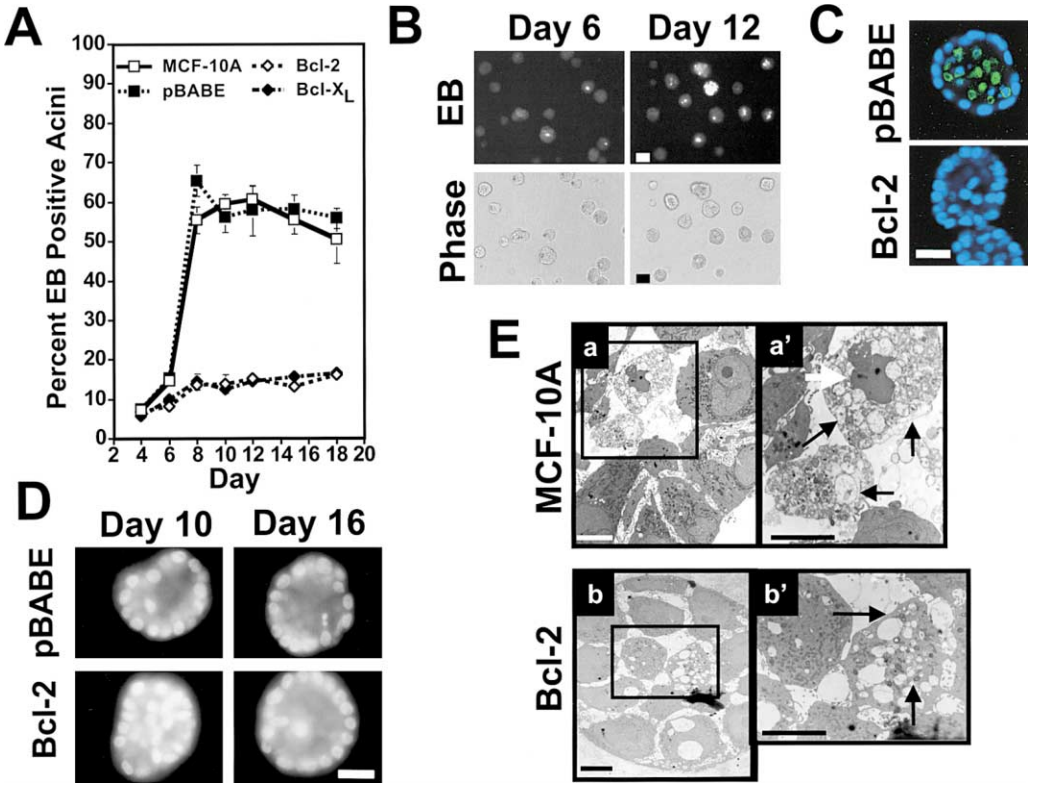

Figure 5. Overexpression of Antiapoptotic Bcl Proteins Decreases Luminal Apoptosis and Delays the Formation of a Hollow Lumen

(A) After the indicated number of days in culture, acini were stained with ethidium bromide (EB) and percentages of acini with EB-positive cells in the lumen were quantified. At least 200 structures were counted for each experiment, and each time point represents the mean ± SEM of five or more independent experiments. Uninfected MCF-10A cells, open squares; pBABE (vector control), filled squares; Bcl-2, open diamonds; Bcl-X_L, filled diamonds.

(B) Representative fields from ethidium bromide-stained MCF-10A acini (EB, top) and corresponding phase (bottom) at the indicated days are shown. Bars equal 50 μm.

(C) Ten-day-old MCF-10A structures expressing pBABE or Bcl-2 were immunostained for activated caspase-3 (green); representative DAPI-stained (blue) crosssections through the equators of acini are shown. Bar equals 25 μm.

(D) Representative DAPI-stained crosssections through the middle of acini overexpressing Bcl-2 (bottom) or vector controls (pBABE, top) are shown at the indicated days. Bar equals 25 μm.

(E) Transmission electron micrographs of day 8 uninfected MCF-10A (a) and Bcl-2-expressing acini (b and c). (a′) and (b′) are enlargements of the boxed areas indicated in (a) and (b). (a) Dying cells are found in the lumen of day 8 MCF-10A (a, boxed area), which exhibit fragmented nuclei (a′, white arrow) and cytoplasmic vacuolation, including autophagic vacuoles (a′, black arrows). (b) Similar vacuoles are observed within cells in day 8 Bcl-2-expressing structures (b′, black arrows). Bars equal 5 μm.

Mammary Acini Expressing Cyclin D1 or HPV 16 E7 Lose Proliferative Suppression but Retain Hollow Lumen

We also investigated the factors that contribute to luminal filling during the morphogenesis of oncogene-expressing mammary structures. As discussed previously, activation of ErbB2 in intact preformed acini using a controlled dimerization strategy resulted in the formation of large multiacinar structures with filled lumen (Muthuswamy et al., 2001). Activation of ErbB2 during the early stages of morphogenesis (starting at day 2 in 3D culture) resulted in structures that were phenotypically similar to those generated by activating ErbB2 in preformed acini; these structures exhibited significant filling of the luminal space (Figure 6A). Moreover, these structures exhibited high levels of cell cycle activity throughout the morphogenetic process (Figure 6A), whereas control structures underwent proliferative arrest.

Since activated ErbB2 structures exhibited such high levels of proliferation, we considered the possibility that increased proliferation was sufficient to produce excess cells within a structure and fill the luminal space. Cyclin D1 is a component of the core cell cycle machinery that facilitates progression through G1 phase of the cell cycle. The *cyclin D1* gene is amplified in approximately 15% of human breast cancers and the protein is overexpressed in over 50% of mammary carcinomas; overexpression of cyclin D1 in mammary epithelium results in increased proliferation (Bartkova et al., 1994; Gillett et al., 1994; Lammie et al., 1991; Schuuring et al., 1992; Wang et al., 1994). We established stable pools of MCF-10A cells overexpressing cyclin D1; when cultured on basement membrane, these cells formed acini that exhibited normal size and morphology, including the presence of a hollow lumen and proper polarization of apical (GM130), lateral (β-catenin), and basal (α6 integrin, collagen 4) markers (Figure 6A and data not shown). Notably,

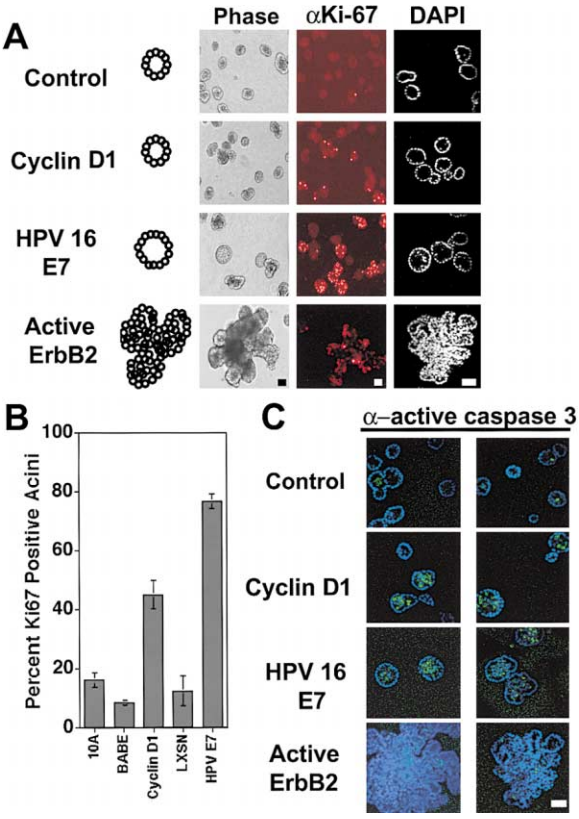

Figure 6. Acini Expressing the Proliferative Oncogenes, Cyclin D1 or HPV 16 E7, Lose Proliferative Suppression but Retain a Hollow Architecture due to Increased Luminal Apoptosis

(A) Morphogenesis of 20-day-old MCF-10A structures expressing cyclin D1 (second row), HPV 16 E7 (third row), or activated ErbB2 (fourth row). The control structures (first row) represent cells infected with the empty vector pBABE. Shown are representative phase contrast images (left column), anti-Ki-67-immunostained structures (red, center column), and DAPI-stained confocal crosssections (right column). Bars equal 50 μm.

(B) Late-stage three-dimensional cultures (days 19–21) of the indicated cell types were immunostained with an antibody against Ki-67 and the percentages of structures with Ki-67-positive cells were quantified. At least 200 acini were counted for each experiment, and the results represent the mean ± SEM from five independent experiments.

(C) 20-day-old structures of the indicated cell types were immunostained with an antibody to activated caspase-3 (green); two representative confocal crosssections through the middle of each structure are shown. Nuclei were counterstained with DAPI (blue). Bar equals 50 μm.

this hollow polarized architecture persisted despite the fact that cells within cyclin D1 acini continued to proliferate, escaping the normal suppression of cell division (Figure 6A); quantification of proliferating acini in late-stage cultures revealed that 50% of the structures contained Ki-67-positive cells, whereas only 10% of controls had evidence of Ki-67 activity (Figure 6B).

The E7 oncoprotein from human papilloma virus 16 (HPV 16 E7) inactivates several key cell cycle regulators, including Rb family proteins and p21, which allows cells to progress through the cell cycle (Munger et al., 2001). Previous work indicates that primary mammary epithelial cells expressing HPV 16 E7 also give rise to structures that fail to growth arrest but retain a polarized morphology (Spancake et al., 1999). This data suggested that increased proliferation is insufficient to disrupt acinar morphology, similar to our observations with cyclin D1. However, in this previous study, the effect of enhanced proliferation on the formation and maintenance of luminal space was not addressed. In order to further evaluate the effects of increased proliferation on luminal filling in mammary acini, we established stable pools of MCF-10A cells expressing HPV 16 E7 and assayed these cells in 3D culture. Cells expressing HPV 16 E7 formed individual acini during morphogenesis. However, these structures were 40% larger than controls; the mean diameter ± standard deviation of HPVE7 acini at day 20 of culture was 93.9 ± 19.5 μm ($n = 110$) versus 67.2 ± 16.5 μm ($n = 103$) of LXSN-expressing controls ($p < 0.001$ using Student's t test).

Nevertheless, acini expressing HPV 16 E7 retained the presence of a hollow lumen and proper polarization, despite the fact that cells within these structures were highly proliferative (Figure 6A). Indeed, during the late stages of the morphogenetic process, up to 80% of the acini expressing E7 had actively dividing cells, whereas the control acini had growth arrested (Figure 6B). The effect of HPV 16 E7 on proliferation was more pronounced than that observed with cyclin D1; in fact, HPV 16 E7-containing structures had significantly increased numbers of Ki-67-positive cells per individual acinar unit, compared to both control and cyclin D1-expressing acini (Figure 6A). These results corroborated those previously obtained with HPV 16 E7 in primary mammary epithelial cells and confirmed that, like decreased apoptosis, increased proliferation within an acinus is not sufficient to elicit luminal space filling.

Further examination of the morphogenesis of these structures revealed that the lumen of acini expressing cyclin D1, and particularly HPV 16 E7, were often notable for large amounts of cellular debris and fragmented nuclei, suggesting that increased cell death was occurring in these structures. Immunostaining for activated caspase-3 confirmed that the luminal spaces within cyclin D1 and HPV 16 E7-expressing acini were filled with apoptotic cells (Figure 6C). As with normal acini, cells in the outer polarized layer of both cyclin D1 and HPV 16 E7 structures remained viable, whereas only cells in the lumen exhibited death. Moreover, we found a striking difference in the extent of luminal apoptosis in structures expressing HPV 16 E7 and cyclin D1 versus those with activated ErbB2; these structures, which exhibited a high degree of luminal filling, had low levels of luminal apoptosis (Figure 6C). Hence, with regard to filling of the luminal space, the phenotypic heterogeneity observed between ErbB2 and the proliferative oncogenes cyclin D1 and HPV 16 E7 is at least partially related to the ability of ErbB2 to provide some protection from luminal apoptosis; cyclin D1 and HPV 16 E7 are unable to provide that protection.

Apoptotic Clearance Is Necessary to Maintain Luminal Space upon Uncontrolled Proliferation within an Acinar Structure

Upon quantifying the percent of acini in a culture exhibiting ethidum bromide-positive cells in the lumen, we

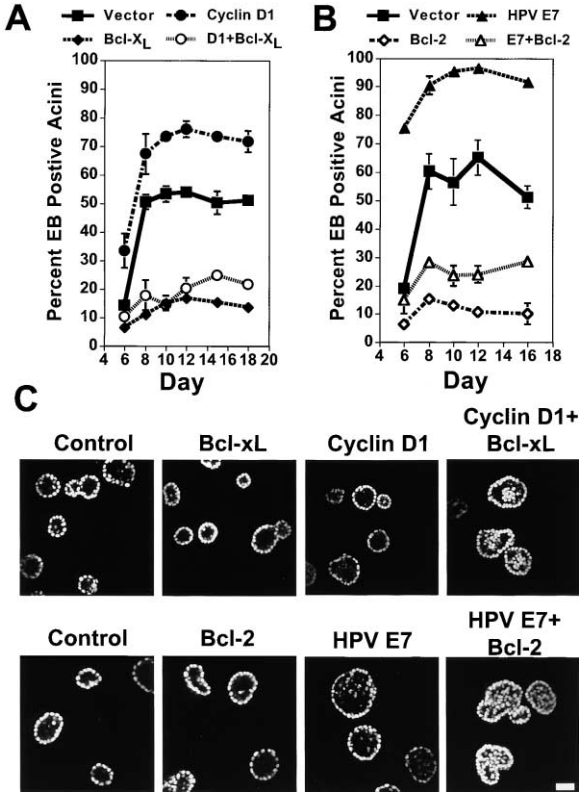

Figure 7. Inhibition of Luminal Apoptosis in Proliferating Structures Results in Population of the Luminal Space

(A and B) The percentages of acini containing ethidium bromide (EB)-positive cells in the lumen were quantified after the indicated days in three-dimensional culture; at least 200 structures were counted for each experiment and each time point represents the mean ± SEM of three to five independent experiments.

(A) Vector control (pBABE), filled squares; Bcl-X_L, filled diamonds; cyclin D1, filled circles; cyclin D1+BclxL, open circles.

(B) Vector control (pBABE+pLXSN), filled squares; Bcl-2, open diamonds; HPV 16 E7, filled triangles; HPV 16 E7+Bcl2, open triangles.

(C) 20-day-old structures of the indicated cell types were fixed and nuclei were stained with DAPI; confocal crosssections through the middles are shown. Bar equals 50 μm.

found that acini expressing either cyclin D1 or HPV 16 E7 showed higher levels of luminal apoptosis compared to vector-infected controls; this increased death was evident throughout the morphogenetic process (Figures 7A and 7B). Remarkably, HPV 16 E7-expressing acini, which demonstrated higher levels of Ki-67 positivity than cyclin D1-expressing structures, also exhibited higher levels of luminal apoptosis, further suggesting that the rate of proliferation within an acinar structure correlated with the rate of luminal apoptosis (Figures 6B, 7A, and 7B). Overall, these results indicated that increased apoptosis can counterbalance increased proliferation within an acinus, resulting in the maintenance of a hollow glandular architecture during morphogenesis.

The above results raised the question whether inhibiting apoptosis would allow excess proliferating cells within an acinus to populate the lumen. In order to address this possibility, we established stable pools of MCF-10A cells expressing a proliferative oncogene combined with an antiapoptotic protein; cells expressing either cyclin D1 with Bcl-X_L or HPV 16 E7 with Bcl-2 were cultured on basement membrane. These structures exhibited significantly lower levels of cell death during morphogenesis, similar to acini expressing antiapoptotic Bcl family proteins alone (Figures 7A and 7B). But, in contrast to acini that express either a proliferative oncoprotein or antiapoptotic protein in isolation, acini expressing both types of proteins exhibited filling of the luminal space, even during the later time points in morphogenesis (Figure 7C). Thus, apoptosis becomes critical in maintaining luminal space when a proliferative stress is imposed by an oncogene like cyclin D1 or HPV 16 E7; luminal filling can only occur when an antiapoptotic or prosurvival signal is combined with a proliferative signal.

Discussion

We have delineated the temporal progression of the biological events that contribute to the morphogenesis of a hollow glandular structure in vitro and have demonstrated that luminal apoptosis is involved in clearance of cells during lumen formation. Surprisingly, blocking apoptosis during acinar morphogenesis by overexpressing antiapoptotic Bcl family proteins can only delay the clearance of cells in the developing lumen; the resulting structures eventually exhibit a hollow architecture. A hollow lumen is also retained when proliferation is enhanced within an acinus due to oncogenes like cyclin D1 or HPV 16 E7; in these structures, increased luminal apoptosis counterbalances increased proliferation to maintain the lumen. Accordingly, the combined disruption of proliferative suppression along with inhibiting cell death elicits filling of the luminal space.

Apoptosis has been observed in the center of cell clusters in both in vitro basement membrane cultures of primary mouse mammary epithelium as well as in the terminal endbuds of the pubertal mouse mammary gland in vivo (Blatchford et al., 1999; Humphreys et al., 1996). However, the precise role of apoptosis in the creation of the lumen in the mammary gland remains unresolved. Transgenic overexpression of Bcl-2 in the mammary gland results in decreased apoptosis in the terminal endbud and disrupts the organization of endbud structures during ductal elongation, yet is not sufficient to completely eliminate lumen formation (Humphreys et al., 1996). Our findings with MCF-10A mammary acini, which demonstrate that inhibiting apoptosis delays but does not eliminate lumen formation, are in accordance with these in vivo studies of ductal morphogenesis.

Several factors may contribute to the ability of Bcl-2- and Bcl-X_L-expressing structures to form a lumen in the absence of apoptosis. As indicated earlier, antiapoptotic Bcl family members are known to have antiproliferative effects in mammary cells; however, we did not observe decreased proliferation due to Bcl-2 or Bcl-X_L overexpression during morphogenesis. Our initial studies of the ultrastructure of developing mammary acini have revealed that the dying cells in the luminal space exhibit large numbers of cytoplasmic vacuoles; some of these vacuoles appear autophagic and are also observed in the centrally located cells of Bcl-2-expressing acini, al-

beit at lower levels. Recently, alternative cell death processes have been recognized in epithelial cells, including autophagy and parapoptosis. (Bursch et al., 2000; Leist and Jaattela, 2001; Sperandio et al., 2000). These pathways can be activated in parallel to apoptosis, and significant crosstalk between apoptotic and alternative death pathways may exist (Lee and Baehrecke, 2001). Thus, autophagic or "type II" cell death may also contribute to the cell clearance during lumen formation. We are currently investigating the role of autophagic death in mammary acinar morphogenesis.

In contrast to normal acini, apoptosis does play a critical role in generating and maintaining the luminal space within proliferating, oncogene-expressing, structures. Upon uncontrolled proliferation within an acinus, luminal apoptosis serves as an important clearance mechanism for excess cells and maintaining a hollow glandular architecture. In human breast cancer pathogenesis, the role and molecular regulation of apoptosis remains unclear. In infiltrating ductal carcinomas and high-grade DCIS, a high apoptotic index has been associated with a high mitotic rate, but it remains unknown if programmed cell death has any effect on the progression and architecture of early oncogenic lesions (Moreno et al., 2001). Our in vitro results demonstrate that increased proliferation within mammary acinar structures must be combined with inhibition of luminal apoptosis to elicit filling of the lumen. Accordingly, the ability of oncogenes like ErbB2 to populate the lumen is at least partially due to their ability to overcome luminal apoptosis. Extrapolating to human tumors, one could speculate that during early carcinoma formation, factors that promote survival in the luminal space can cooperate with a proliferative oncogene to produce a more advanced phenotype.

The increased luminal apoptosis we have observed in structures expressing cyclin D1 and HPV E7 may reflect the ability of these oncoproteins to promote apoptotic pathways. Cyclin D1 and HPV E7 can both inhibit the tumor suppressor functions of retinoblastoma (Rb) family proteins, resulting in increased activity of E2F transcription factors (Munger et al., 2001; Sherr, 1996). Multiple genes involved in apoptosis are known E2F targets (Muller and Helin, 2000). Moreover, it is known that other oncogenes like c-*myc* display proapoptotic activity and that tumor progression requires suppression of this apoptotic activity (Evan et al., 1992; Pelengaris et al., 2002). Whether luminal apoptosis within oncogene-expressing structures represents an intrinsic clearance mechanism in proliferating structures or a manifestation of proapoptotic pathways activated by oncogenes is an important issue for further study. In either case, our studies provide the first evidence that circumventing apoptosis is an important barrier for cancer genes to overcome in order to populate the lumen of glandular structures.

A salient aspect of our results is that cell death is always confined to the luminal space, even in proliferating, oncogene-expressing structures. Thus, it is important to elucidate the mechanisms that are responsible for the selective death of cells in the center of acini. Our initial studies illustrate that Akt pathway is preferentially activated in the matrix-attached cells occupying the periphery of each structure. Akt may promote survival of cells by diverse mechanisms, including phosphorylation-mediated inactivation of proapoptotic proteins such as Bad, the transcriptional repression of proapoptotic genes, and improved glucose metabolism and mitochondrial homeostasis due to enhanced glucose uptake and glycolysis (Brunet et al., 1999; Datta et al., 1997, 1999; Plas et al., 2001). One can hypothesize that the inner cells lacking basement membrane contact cannot transduce this wide array of Akt-mediated survival signals, and thus become susceptible to *anoikis*, a form of programmed cell death that epithelial cells undergo upon detachment from extracellular matrix (Boudreau et al., 1995; Frisch et al., 1996). Evidence from our laboratory indicates that several molecules involved in *anoikis* in MCF-10A cells are also important regulators of luminal apoptosis in mammary acini, consistent with the role of *anoikis* in luminal apoptosis (M.J.R., K.R.M., and J.S.B., unpublished data).

It is also possible that the induction of lumen formation involves an active morphogenetic process, associated with the polarization of basement membrane-attached cells, rather than simply *anoikis*. In periimplantation mouse blastocysts, epiblast cells in contact with basement membrane polarize to form a layer of columnar epithelium, whereas unpolarized cells in the center die, giving rise to the proamniotic cavity (Coucouvanis and Martin, 1995; Murray and Edgar, 2000). Two signals mediate this cavitation—an active death signal that triggers the demise of cells in the cavity and a survival signal that protects cells lining the cavity (Coucouvanis and Martin, 1995, 1999). Notably, the absence of basement membrane prevents cell polarization (but not differentiation) and abolishes cell death and cavity formation in blastocysts (Murray and Edgar, 2000). In MCF-10A acini, we have demonstrated that apicobasal polarity is established during early morphogenesis, whereupon a layer of cells within each structure is polarized and a second unorganized population remains in the center; this event precedes both apoptosis and lumen formation. Further experiments are needed to establish a definite causal relationship between the initial polarization and the subsequent onset of luminal apoptosis in MCF-10A acini.

Nevertheless, since apicobasal polarization of cells is an early event in acini development, one can speculate that a cancer gene that disrupts polarity may have profound effects on luminal space and glandular structure, either on its own or in cooperation with other insults like increased proliferation or decreased apoptosis. Recent studies in *Drosophila* have shown that disruption of genes controlling cell polarity, including *Dlg*, *Scrib*, and *Lgl*, elicits hyperplastic growth (Bilder et al., 2000). Also, we have previously shown that activation of ErbB2 disrupts cell polarity in MDCK polarized monolayers; this loss of polarity may also contribute to the multiacinar phenotype produced upon activating ErbB2 in 3D culture (Muthuswamy et al., 2001). However, the role of polarity on tumor progression could be complex; recent studies in three-dimensional culture indicate that the disrupting polarization renders both normal and malignant mammary epithelial structures susceptible to apoptosis upon treatment with death-inducing agents (Weaver et al., 2002).

In summary, we have demonstrated that apoptosis contributes to a key aspect of mammary acinar morpho-

genesis, the generation and maintenance of a hollow lumen. Notably, this hollow lumen can be retained upon either enhancing proliferation or decreasing apoptosis within developing acini, suggesting that epithelial architecture is relatively resistant to isolated biological insults imposed by cancer genes. However, the combined disruption of proliferative suppression and luminal apoptosis does fill the lumen. Furthermore, oncogenes that are able to exert multiple biological effects, such as ErbB2, give rise to more advanced phenotypes in this system. Overall, these results point to the utility of three-dimensional culture systems in modeling the biological activities of cancer genes, particularly with regard to their ability to disrupt epithelial architecture.

Experimental Procedures

Materials

MCF-10A cells were obtained from ATCC (Manassas, Virginia) and cultured in DMEM/F12 (Invitrogen) supplemented with 5% donor horse serum, 20 ng/ml epidermal growth factor (EGF), 10 μg/ml insulin, 100 μg/ml hydrocortisone, 1 ng/ml cholera toxin, 50 U/ml penicillin, and 50 mg/ml streptomycin. Growth factor-reduced Matrigel™ (BD Biosciences) lots with protein concentrations between 9 and 11 mg/ml were used. Anti-α_6 integrin and human-specific anti-laminin V antibodies were obtained from Chemicon; anti-β-catenin, anti-E-cadherin, and anti-GM130 from BD Transduction; anti-Ki-67 from Zymed; anti-activated caspase-3, anti-activated caspase-9, anti-phospho-Akt Ser473 (IHC Specific), and anti-phospho-Akt substrate from Cell Signaling Technologies; and human-specific anti-Collagen IV from DAKO.

Retroviral Vectors and Virus Production

pBABEpuro Bcl-2 and pBABEhygro Bcl-X_L cDNAs were a gift from Drs. Or Gozani and Junying Yuan (Harvard Medical School). pBABEpuro cyclin D1 was constructed by inserting a BamH1 fragment from pFLEX cyclin D1 (a gift from Alan Diehl, University of Pennsylvania) into the Bam H1 site of pBABEpuro. VSV-pseudotyped retroviruses were produced by transfection of the VSV-GPG producer cell line (Ory et al., 1996) with 15 μg of DNA using Lipofectamine™ (Invitrogen). Retrovirus-containing supernatants were collected at days 5 through 7 following transfection and were stored at −80°C. Retroviral vectors encoding the HPV 16 E7 viral oncoprotein and the empty vector (pLXSN) were produced from the cell lines PA317-16E7 and PA317-LXSN, respectively, that were obtained as a gift from Drs. Denise Galloway (Fred Hutchinson Cancer Research Center) and Peter Howley (Harvard Medical School) (Halbert et al., 1991).

Generation of MCF-10A Cell Lines

MCF-10A cells were plated at 4×10^5 cells per 10 cm dish and infected with the retroviruses above, and stable populations were obtained by selection with 2 μg/ml puromycin (Sigma), 200 μg/ml hygromycin (Calbiochem), or 200 μg/ml active G418 (Sigma). Stable pools of MCF-10A cells that coexpressed HPV16 E7 and Bcl-2 were generated by serially infecting with HPV16 E7 retrovirus, followed by pBABEpuro Bcl-2; stable pools coexpressing cyclin D1 with Bcl-X_L were obtained by serial infection of pBABEpuro Cyclin D1 followed by pBABEhygro Bcl-X_L. Stable MCF-10A cells containing p75.B2, a chimeric ErbB2 receptor fused to the bivalent ligand FK-506 binding protein (FKBP), and its activation via dimerization with the bivalent ligand AP1510 (ARIAD Pharmaceuticals) have been previously described (Muthuswamy et al., 1999, 2001).

Protein expression was confirmed by immunoblotting using the following antibodies: anti-Bcl-2 (Santa Cruz), anti-Bcl-X_L (BD Pharmingen), anti-cyclin D1 (Santa Cruz), and anti-HPV 16 E7 (Zymed). The biochemical activity of HPV 16 E7 was also confirmed by decreased levels of retinoblastoma protein (Rb), which was determined by immunoblotting with anti-Rb (BD Pharmingen); degradation of Rb protein occurs in the presence of E7 (Boyer et al., 1996).

Morphogenesis Assay

The three-dimensional culture of MCF-10A cells on basement membrane was carried out as previously described (Muthuswamy et al., 2001) with the following two modifications. Assay medium (DMEM/F12 supplemented with 2% donor horse serum, 10 μg/ml insulin, 1 ng/ml cholera toxin, 100 μg/ml hydrocortisone, 50 U/ml penicillin, and 50 μg/ml streptomycin) containing 5 ng/ml EGF and 2% Matrigel was replaced every 4 days. For stimulation of cells containing ErbB2 chimeras with AP1510, the EGF-containing assay medium was replaced with assay medium containing 1 μM AP1510 on day 2; as before, cultures were refed every 4 days with assay media containing AP1510.

Immunofluorescence Analysis and Image Acquisition

Acinar structures were fixed in 2% formalin (Sigma) at room temperature for 25 min and permeabilized in 0.5% Triton X-100 in PBS for 10 min at 4°C. Except for this minor modification in fixation and permeablization, the immunostaining of acinar structures was carried out as previously described (Muthuswamy et al., 2001). Indirect immunofluorescence was performed on a Nikon TE300 microscope equipped with a mercury lamp and CCD camera; images were acquired using IP Lab Spectrum (version 3.1). Confocal analyses were performed using the Zeiss LSM410 confocal microscopy system equipped with krypton-argon (488 and 568 lines) and ultraviolet (365 line) lasers; images were acquired using LSM version 3.99. For each time point, the images presented are representative of four or more independent experiments. All images were converted to TIFF format and arranged using Photoshop 5.0.

Transmission Electron Microscopy

Acini were cultured on basement membrane, fixed (1.2% paraformaldehyde, 2.5% gluteraldehyde, 0.03% picric acid in 100 mM cacodylate buffer), and submitted to the Harvard Medical School Electron Microscopy facility for processing and image acquisition (JEOL 1200EX). Detailed protocols are available at http://cellbio.med.harvard.edu/research/facilities/electron_microscopy/conventional.html.

In Situ Live/Dead Cell Analysis and Quantification of Cell Death in Mammary Acini

Assay media was removed from wells and acini were washed once with PBS. Structures were then incubated for 15–30 min at 37°C with a mixture of 1 μM ethidium bromide (EtBr) and 5 μM calcein AM (Molecular Probes) in PBS. Indirect immunofluorescence was performed on a Nikon TE300 microscope as above. For quantification of cell death within acini, cultures at various time points were stained with 1 μM ethidium bromide for 15 min. The percent of acini containing one or more ethidium bromide-positive cell was counted using a Nikon Eclipse TE300 microscope.

Determination of Acinar Permeability to High-Molecular-Weight Dextrans

High-molecular-weight dextrans (3,000, 10,000, or 40,000 MW) conjugated to fluorescein (Molecular Probes) were added to cultures at 5 μg/ml in assay media. Acini were treated for 37°C for 30 min, washed briefly with PBS, mounted with 1:1 PBS:glycerol, and immediately analyzed by confocal microscopy to determine extent of dextran entry into the luminal spaces.

Acknowledgments

We thank Dr. Mina Bissell for stimulating discussions on this work and Dr. Peter Howley for critical reading of the manuscript. We also thank Drs. Or Gozani, Junying Yuan, Denise Galloway, Peter Howley, and Alan Diehl for various reagents indicated in Experimental Procedures; Richard Mulligan for the 293-GPG retrovirus packaging line; Maria Ericsson for assistance with electron microscopy; and Terry Keenan and ARIAD Pharmaceuticals for providing AP1510 (www.ariad.com/regulationkits). This work was supported by grants from National Cancer Institute (CA80111; CA89393), Aventis Pharmaceuticals, and American Cancer Society (to J.S.B.); an HHMI Physician Postdoctoral Fellowship (to J.D.); a Susan Komen Breast Cancer Postdoctoral Fellowship (to M.J.R.); a Massachusetts Public Health Breast

Cancer Research Award (to S.K.M.); and National Science Foundation Graduate Research Fellowships (to K.R.M. and N.L.C.).

Received: June 26, 2002
Revised: August 30, 2002

References

Bartkova, J., Lukas, J., Muller, H., Lutzhoft, D., Strauss, M., and Bartek, J. (1994). Cyclin D1 protein expression and function in human breast cancer. Int. J. Cancer *57*, 353–361.

Bilder, D., Li, M., and Perrimon, N. (2000). Cooperative regulation of cell polarity and growth by *Drosophila* tumor suppressors. Science *289*, 113–116.

Bissell, M.J., and Radisky, D. (2001). Putting tumours in context. Nat. Rev. Cancer *1*, 46–54.

Blatchford, D.R., Quarrie, L.H., Tonner, E., McCarthy, C., Flint, D.J., and Wilde, C.J. (1999). Influence of microenvironment on mammary epithelial cell survival in primary culture. J. Cell. Physiol. *181*, 304–311.

Boudreau, N., Sympson, C.J., Werb, Z., and Bissell, M.J. (1995). Suppression of ICE and apoptosis in mammary epithelial cells by extracellular matrix. Science *267*, 891–893.

Boyer, S.N., Wazer, D.E., and Band, V. (1996). E7 protein of human papilloma virus-16 induces degradation of retinoblastoma protein through the ubiquitin-proteasome pathway. Cancer Res. *56*, 4620–4624.

Brunet, A., Bonni, A., Zigmond, M.J., Lin, M.Z., Juo, P., Hu, L.S., Anderson, M.J., Arden, K.C., Blenis, J., and Greenberg, M.E. (1999). Akt promotes cell survival by phosphorylating and inhibiting a Forkhead transcription factor. Cell *96*, 857–868.

Bursch, W., Ellinger, A., Gerner, C., Frohwein, U., and Schulte-Hermann, R. (2000). Programmed cell death (PCD). Apoptosis, autophagic PCD, or others? Ann. N Y Acad. Sci. *926*, 1–12.

Coucouvanis, E., and Martin, G.R. (1995). Signals for death and survival: a two-step mechanism for cavitation in the vertebrate embryo. Cell *83*, 279–287.

Coucouvanis, E., and Martin, G.R. (1999). BMP signaling plays a role in visceral endoderm differentiation and cavitation in the early mouse embryo. Development *126*, 535–546.

Datta, S.R., Dudek, H., Tao, X., Masters, S., Fu, H., Gotoh, Y., and Greenberg, M.E. (1997). Akt phosphorylation of BAD couples survival signals to the cell-intrinsic death machinery. Cell *91*, 231–241.

Datta, S.R., Brunet, A., and Greenberg, M.E. (1999). Cellular survival: a play in three Akts. Genes Dev. *13*, 2905–2927.

Evan, G.I., Wyllie, A.H., Gilbert, C.S., Littlewood, T.D., Land, H., Brooks, M., Waters, C.M., Penn, L.Z., and Hancock, D.C. (1992). Induction of apoptosis in fibroblasts by c-myc protein. Cell *69*, 119–128.

Frisch, S.M., Vuori, K., Ruoslahti, E., and Chan-Hui, P.Y. (1996). Control of adhesion-dependent cell survival by focal adhesion kinase. J. Cell Biol. *134*, 793–799.

Furth, P.A., Bar-Peled, U., Li, M., Lewis, A., Laucirica, R., Jager, R., Weiher, H., and Russell, R.G. (1999). Loss of anti-mitotic effects of Bcl-2 with retention of anti-apoptotic activity during tumor progression in a mouse model. Oncogene *18*, 6589–6596.

Gillett, C., Fantl, V., Smith, R., Fisher, C., Bartek, J., Dickson, C., Barnes, D., and Peters, G. (1994). Amplification and overexpression of cyclin D1 in breast cancer detected by immunohistochemical staining. Cancer Res. *54*, 1812–1817.

Gudjonsson, T., Ronnov-Jessen, L., Villadsen, R., Rank, F., Bissell, M.J., and Petersen, O.W. (2002). Normal and tumor-derived myoepithelial cells differ in their ability to interact with luminal breast epithelial cells for polarity and basement membrane deposition. J. Cell Sci. *115*, 39–50.

Halbert, C.L., Demers, G.W., and Galloway, D.A. (1991). The E7 gene of human papillomavirus type 16 is sufficient for immortalization of human epithelial cells. J. Virol. *65*, 473–478.

Harris, J., Lippman, M., Morrow, M., and Osborne, C. (1999). Diseases of the Breast (Philadelphia, PA: Lippincott Williams and Wilkins).

Hoffman, M.P., Kibbey, M.C., Letterio, J.J., and Kleinman, H.K. (1996). Role of laminin-1 and TGF-beta 3 in acinar differentiation of a human submandibular gland cell line (HSG). J. Cell Sci. *109*, 2013–2021.

Humphreys, R.C., Krajewska, M., Krnacik, S., Jaeger, R., Weiher, H., Krajewski, S., Reed, J.C., and Rosen, J.M. (1996). Apoptosis in the terminal endbud of the murine mammary gland: a mechanism of ductal morphogenesis. Development *122*, 4013–4022.

Korff, T., and Augustin, H.G. (1998). Integration of endothelial cells in multicellular spheroids prevents apoptosis and induces differentiation. J. Cell Biol. *143*, 1341–1352.

Lammie, G.A., Fantl, V., Smith, R., Schuuring, E., Brookes, S., Michalides, R., Dickson, C., Arnold, A., and Peters, G. (1991). D11S287, a putative oncogene on chromosome 11q13, is amplified and expressed in squamous cell and mammary carcinomas and linked to BCL-1. Oncogene *6*, 439–444.

Lee, C.Y., and Baehrecke, E.H. (2001). Steroid regulation of autophagic programmed cell death during development. Development *128*, 1443–1455.

Leist, M., and Jaattela, M. (2001). Four deaths and a funeral: from caspases to alternative mechanisms. Nat. Rev. Mol. Cell Biol. *2*, 589–598.

Manning, B.D., Tee, A.R., Logsdon, M.N., Blenis, J., and Cantley, L.C. (2002). Identification of the tuberous sclerosis complex-2 tumor suppressor gene product tuberin as a target of the phosphoinositide 3-kinase/akt pathway. Mol. Cell *10*, 151–162.

Moreno, A., Figueras, A., Lloveras, B., Escobedo, A., Griera, E., Sierra, A., and Fabra, A. (2001). Apoptosis in ductal carcinoma in situ of the breast. Breast J. *7*, 245–248.

Muller, H., and Helin, K. (2000). The E2F transcription factors: key regulators of cell proliferation. Biochim. Biophys. Acta *1470*, M1–M12.

Munger, K., Basile, J.R., Duensing, S., Eichten, A., Gonzalez, S.L., Grace, M., and Zacny, V.L. (2001). Biological activities and molecular targets of the human papillomavirus E7 oncoprotein. Oncogene *20*, 7888–7898.

Murphy, K.L., Kittrell, F.S., Gay, J.P., Jager, R., Medina, D., and Rosen, J.M. (1999). Bcl-2 expression delays mammary tumor development in dimethylbenz(a)anthracene-treated transgenic mice. Oncogene *18*, 6597–6604.

Murray, P., and Edgar, D. (2000). Regulation of programmed cell death by basement membranes in embryonic development. J. Cell Biol. *150*, 1215–1221.

Muthuswamy, S.K., Gilman, M., and Brugge, J.S. (1999). Controlled dimerization of ErbB receptors provides evidence for differential signaling by homo- and heterodimers. Mol. Cell. Biol. *19*, 6845–6857.

Muthuswamy, S.K., Li, D., Lelièvre, S., Bissell, M.J., and Brugge, J.S. (2001). ErbB2, but not ErbB1, reinitiates proliferation and induces luminal repopulation in epithelial acini. Nat. Cell Biol. *3*, 785–792.

O'Brien, L.E., Zegers, M.M., and Mostov, K.E. (2002). Opinion: building epithelial architecture: insights from three-dimensional culture models. Nat. Rev. Mol. Cell Biol. *3*, 531–537.

Ojakian, G.K., Nelson, W.J., and Beck, K.A. (1997). Mechanisms for de novo biogenesis of an apical membrane compartment in groups of simple epithelial cells surrounded by extracellular matrix. J. Cell Sci. *110*, 2781–2794.

Ory, D.S., Neugeboren, B.A., and Mulligan, R.C. (1996). A stable human-derived packaging cell line for production of high titer retrovirus/vesicular stomatitis virus G pseudotypes. Proc. Natl. Acad. Sci. USA *93*, 11400–11406.

Pelengaris, S., Khan, M., and Evan, G.I. (2002). Suppression of myc-induced apoptosis in Beta cells exposes multiple oncogenic properties of myc and triggers carcinogenic progression. Cell *109*, 321–334.

Petersen, O.W., Ronnov-Jessen, L., Howlett, A.R., and Bissell, M.J. (1992). Interaction with basement membrane serves to rapidly distinguish growth and differentiation pattern of normal and malignant human breast epithelial cells. Proc. Natl. Acad. Sci. USA *89*, 9064–9068.

Plas, D.R., Talapatra, S., Edinger, A.L., Rathmell, J.C., and Thompson, C.B. (2001). Akt and Bcl-xL promote growth factor-independent survival through distinct effects on mitochondrial physiology. J. Biol. Chem. *276*, 12041–12048.

Scholzen, T., and Gerdes, J. (2000). The Ki-67 protein: from the known and the unknown. J. Cell. Physiol. *182*, 311–322.

Schuuring, E., Verhoeven, E., Mooi, W.J., and Michalides, R.J. (1992). Identification and cloning of two overexpressed genes, U21B31/PRAD1 and EMS1, within the amplified chromosome 11q13 region in human carcinomas. Oncogene *7*, 355–361.

Sherr, C.J. (1996). Cancer cell cycles. Science *274*, 1672–1677.

Soule, H.D., Maloney, T.M., Wolman, S.R., Peterson, W.D., Jr., Brenz, R., McGrath, C.M., Russo, J., Pauley, R.J., Jones, R.F., and Brooks, S.C. (1990). Isolation and characterization of a spontaneously immortalized human breast epithelial cell line, MCF-10. Cancer Res. *50*, 6075–6086.

Spancake, K.M., Anderson, C.B., Weaver, V.M., Matsunami, N., Bissell, M.J., and White, R.L. (1999). E7-transduced human breast epithelial cells show partial differentiation in three-dimensional culture. Cancer Res. *59*, 6042–6045.

Sperandio, S., de Belle, I., and Bredesen, D.E. (2000). An alternative, nonapoptotic form of programmed cell death. Proc. Natl. Acad. Sci. USA *97*, 14376–14381.

Streuli, C.H., and Bissell, M.J. (1990). Expression of extracellular matrix components is regulated by substratum. J. Cell Biol. *110*, 1405–1415.

Wang, T.C., Cardiff, R.D., Zukerberg, L., Lees, E., Arnold, A., and Schmidt, E.V. (1994). Mammary hyperplasia and carcinoma in MMTV-cyclin D1 transgenic mice. Nature *369*, 669–671.

Watton, S.J., and Downward, J. (1999). Akt/PKB localisation and 3′ phosphoinositide generation at sites of epithelial cell-matrix and cell-cell interaction. Curr. Biol. *9*, 433–436.

Weaver, V.M., Lelièvre, S., Lakins, J.N., Chrenek, M.A., Jones, J.C.R., Giancotti, F., Werb, Z., and Bissell, M.J. (2002). β4 integrin-dependent formation of polarized three-dimensional architecture confers resistance to apoptosis in normal and malignant mammary epithelium. Cancer Cell *2*, 205–216.